NANO LETTERS

2005
Vol. 5, No. 7
1361−1365

Femtosecond Laser Nanosurgery of Defects in Carbon Nanotubes

Aldo H. Romero

CINVESTAV Querétaro, Libramiento Norponiente No 2000, 76230 Querétaro, Mexico

Martin E. Garcia*

Theoretische Physik, Fachbereich Naturwissenschaften, Universität Kassel, and Center for Interdisciplinary Nanostructure Science and Technology (CINSaT), Heinrich-Plett-Str. 40, 34132, Kassel, Germany

Felipe Valencia, Humberto Terrones, and Mauricio Terrones

Advanced Materials Department, IPICYT, Camino Presa San José 2055, 78216, San Luis Potosí, S.L.P., Mexico

Harald O. Jeschke

Institut für theoretische Physik, Johann Wolfgang Goethe-Universität, Max-von-Laue-Str. 1, 60438 Frankfurt/Main, Germany

Received April 3, 2005; Revised Manuscript Received June 9, 2005

ABSTRACT

All self-assembled nanostructures, like carbon nanotubes, exhibit structural imperfections that affect their electronic and mechanical properties and constitute a serious problem for the development of novel electronic nanodevices. Very common defects in nanotubes are pentagon–heptagon pairs, in which the replacement of four hexagons by two pentagons and two heptagons disrupts the perfect hexagonal lattice. In this work, we demonstrate that these defects can be eliminated efficiently with the help of femtosecond laser pulses. By performing nonadiabatic molecular dynamics simulations, we show that in the laser-induced electronic nonequilibrium the pentagon–heptagon pair is transformed back into four hexagons without producing any irreversible damage to the rest of the nanotube.

The presence of subnanometer-scale lattice imperfections has been demonstrated in different nanostructures.[1,2] The fascinating properties of carbon nanotubes (CNTs), which are considered excellent candidates for the construction of electronic nanodevices,[3] can be affected dramatically by the presence of pentagon−heptagon (5−7) pair defects.[4,5,6,7] Therefore, the development of methods able to manipulate such small defects is vital. We have performed a series of nonadiabatic molecular dynamics simulations dealing with the action of strong laser pulses on 5−7−5−7 defects embedded in the hexagonal lattice of single-walled carbon nanotubes (SWNTs). We found that femtosecond lasers eliminate lattice imperfections efficiently by inducing a nonthermal transition occurring at low lattice temperatures. We demonstrate for the first time that femtosecond laser pulses could manipulate atomic-scale defects in nanostructures.

The ability of femtosecond laser pulses to manipulate structures is based on the fact that they are active on the time scales of lattice motion and change the potential landscape abruptly through the excitation of a large fraction ξ of the valence electrons. The nonequilibrium states created by the laser pulse are characterized by extremely high electron temperatures and low kinetic energy of the atoms. Recently, different kinds of laser-induced ultrafast phase transitions have been reported for other systems.[8,9]

Our treatment consists of a nonadiabatic MD method that takes into account, on a microscopic level, the laser excitation and thermalization processes suffered by the electrons and their influence on the lattice dynamics. The method has been described in detail in refs 10 and 11.

To properly describe the laser-induced structural changes, we consider the dynamics of the atoms moving on a time-dependent potential energy surface (PES) $U[\{r_{ij}\}, \{n_l(t)\}] = V_e[\{r_{ij}\}, \{n_l(t)\}] - T_e S_e[\{n_l(t)\}]$, obtained as the free energy of the electrons. V_e is the electronic energy, obtained from the diagonalization of a tight-binding (TB) Hamiltonian with distance-dependent hopping matrix elements and core−core repulsive terms. S_e is the electronic entropy, and $T_e(t)$ is the

* Corresponding author. E-mail: garcia@physik.uni-kassel.de.

10.1021/nl050626t CCC: $30.25
Published on Web 06/24/2005

electronic temperature. $\{r_{ij}\}$ are the interatomic distances, and $\{n_l(t)\}$ are the time-dependent occupations of the electronic levels of the TB Hamiltonian. A time-dependent laser field of shape, $E(t)$, and frequency, ω, excites the system, consequently changing the electronic occupations, n_l. The time-derivatives of the n_l's satisfy coupled equations that are derived from the equation of motion for the reduced density matrix of the electronic system. The laser pulse changes the initial ground-state electronic distribution, $n_l(\mu_0, T_0)$, into a time-dependent nonequilibrium distribution, $n_l(t)$, which then converges, because of electron−electron collisions, to a Fermi-like function, $n_l(\mu, T_e)$. $\mu(t)$ is the chemical potential. The forces, $\boldsymbol{F}_i$, acting on the ith ion must be determined in order to perform MD simulations. This is done by computing $\boldsymbol{F}_i(t) = -\nabla_i U[\{r_{ij}\}, \{n_l(t)\}]$. The TB parameters and their distance dependencies are obtained from ref 12.

The CNT was initially equilibrated to 300 K. Then, a laser pulse with a central frequency of $\hbar\omega = 1.96$ eV was applied. The frequency was chosen to meet that experimentally used on nanotubes.[13] Moderate variations around this value do not lead to qualitative changes in the results. The electron−lattice relaxation time, τ_2, was 4.4 ps,[10] and an electron thermalization time of $\tau_1 = 50$ fs was used. The variables in our calculations are the absorbed energy per atom and the type of tube considered (zigzag or armchair).

We performed calculations on (7, 7) zigzag and (12, 0) armchair CNT with at least 240 atoms in a supercell geometry. Two different boundary conditions were considered: (i) variable supercell[14] and (ii) fixed supercell. The first condition simulates the situation in which the laser spot is larger than the CNT, which can thus expand rapidly as a consequence of the excitation. The second condition is valid when the CNT is larger than the spot. In this case, because the mechanical propagation in the unexcited part of the CNT is limited by the sound velocity, no longitudinal volume changes occur on subpicosecond time scales.

We considered a single-wall nanotube possessing an individual 5−7−5−7 defect within the supercell, corresponding to a defect density of 3% because of the periodic boundary conditions. This defect is caused by a Stone−Wales-type transformation, that is, the 90° rotation of a carbon bond that turns four hexagons of the SWNT into two pentagons and two heptagons (see top panel of Figure 1). It has been demonstrated that, once this defect is formed, an energy barrier of the order of 4−6 eV needs to be overcome to return to the perfect lattice in the case of graphite or a fullerene.[15,16] In Figure 1, we demonstrate that femtosecond laser pulses are suited to eliminate such structural defects efficiently by inverting a generalized Stone−Wales transformation (GSW).[6] The first remarkable feature in the time evolution of the CNT upon excitation is the presence of a coherent phonon corresponding to a large amplitude radial breathing mode (RBM).[17] During the first 400 fs, this leads to reversible bond breaking and reconstruction processes around the pentagon−heptagon defect. Then, the laser-induced change of the potential landscape, U, starts to be appreciable, in particular in the defect region. The two atoms building the dimer involved in the Stone−Wales-type transformation move together, keeping their interatomic distance approximately constant, and breaking their bonds with the surrounding atoms. During this process, which starts about 400 fs after the pulse maximum, the dimer performs a complex motion that has a component in the direction perpendicular to the nanotube wall and an "in-plane" one. This motion ends up with the elimination of the 5−7−5−7 defect and the healing of the CNT. The final result of the trajectory of the dimer is an effective 90° rotation in the wall. An ultrafast inverse SW-type transformation has occurred, induced by the femtosecond laser excitation. It is worth noting that after the laser excitation and during the whole transition shown in Figure 1 the lattice temperature remained low ($T_L < 450$ K), making this a typical example of a nonthermal structural transition.

We have investigated the universality of the described defect healing effect by studying (7, 7) and (12, 0) SWNTs for different parameters of the laser pulse and by inducing the inverse SW transition in a graphene sheet, which could be viewed as the infinite diameter SWNT limit.[18] Furthermore, we found that the same kind of dimer rotation cannot be observed in C_{60}. In the following, we show that the SW healing effect relies on the excitation of 7% of the electrons, leading to strong vibrational excitation in the defect region and to a suppression of the barrier against the inverse SW rotation because of the high electronic entropy. Thus, we conclude that the described effect is not limited to details of the density of states (DOS) close to the Fermi level (i.e., metallic or semiconducting DOS) but is in fact a universal effect. In fact, this effect may have been observed in experiment albeit without clarification of the microscopic origin: Corio et al.[13] find 10-fold increased resonant Raman intensity after excitation of a SWNT bundle with an intense laser pulse and ascribe this to laser annealing of the SWNTs, leading to less structural disorder and thus a more ideal 1D electronic system.

To characterize the motion of the dimer described above, we plot angles φ_{dimer} and ϑ_{dimer} in Figure 2, describing the "in-wall" and "out-of-wall" trajectory of the dimer. The laser-induced inverse SW-type transformation starts at $\vartheta_{dimer} = \varphi_{dimer} = 0°$ and after some oscillations there is a monotonic increase of φ_{dimer}, while ϑ_{dimer} reaches a maximum at ∼55°. This intermediate structure represents the transition state in the way from the 5−7−5−7 defect to the pure CNT. The final state obviously corresponds to $\vartheta_{dimer} = 0°$ and $\varphi_{dimer} = 90°$. The out-of-wall motion of the dimer is a feature inherent of the laser-induced transition, as we show below.

To understand the mechanism and identify the driving force for this nonthermal structural change, we plot in Figure 3 the free energy of the electrons along the transition trajectory corresponding to the structures shown in Figure 1, but assuming different (fixed) electronic temperatures. Figure 3a shows $U(T_e)$ along the initial part of the trajectory, between the pulse maximum and 200 fs. For low T_e, there is an initial increase of the potential energy during the radial expansion of the nanotube caused by the RBM. The increase in U is due to the fact that the expansion causes bond-

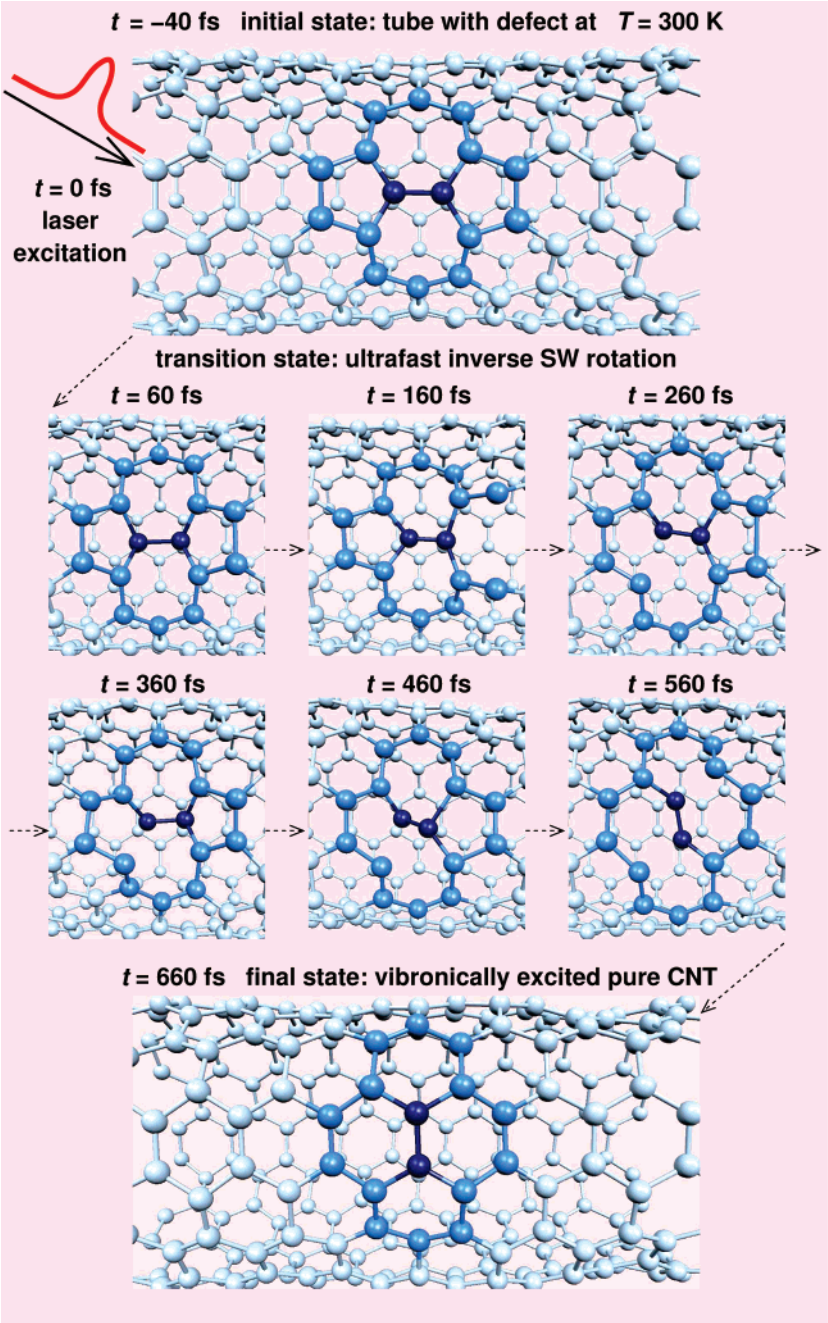

Figure 1. Snapshots of the response of a (7, 7)-CNT to a femtosecond laser pulse of 50 fs duration (of Gaussian shape) leading to the elimination of the pentagon−heptagon defect. The defect region is marked in saturated blue, with the SW dimer colored in dark blue. Bonds are drawn between atoms closer than 2 Å. The energy absorbed by the CNT was 1.7 eV/atom, considerably below the threshold energy for this diameter, that is, the energy to create one or more irreversible bond-breaking processes. Top panel: Entire simulated SWNT section with 5−7−5−7 defect before the action of the pulse (time is measured with respect to the pulse maximum). Center panel: Reversible bond-breaking processes in the vicinity of the SW dimer take place from $t = 60$ fs to $t = 260$ fs, and the inverse Stone−Wales-type transformation occurs from $t = 360$ fs to $t = 560$ fs. Bottom panel: At $t = 660$ fs, the perfect SWNT has been restored.

breaking processes around the 5−7−5−7 defect, which costs energy. However, for $T_e > 20\,000$ K, the radial expansion of the CNT does not cost energy any more, and for higher T_e the initial SW state becomes *unstable*. It is important to mention that the electronic energy $V_e(T_e > 20\,000\ \text{K})$ does not show any instabilities at the initial SW state. Thus, it is clear that the ultrafast structural transition shown in Figures 1 and 2 is driven by the increase of the electronic entropy produced by the laser excitation.

In Figure 3b, we show the behavior of $U(T_e)$ along the part of the trajectory where the inverse SW-type transformation occurs (between 450 and 600 fs after the pulse maximum). Again, a decrease of the barrier for the dimer rotation is observed for increasing electronic temperature. The barrier is suppressed for $T_e > 20\,000$ K. This is due to the dramatic effect of the electronic entropy.

We performed calculations at different laser intensities for the (7, 7) zigzag CNT and the (12, 0) armchair CNT with

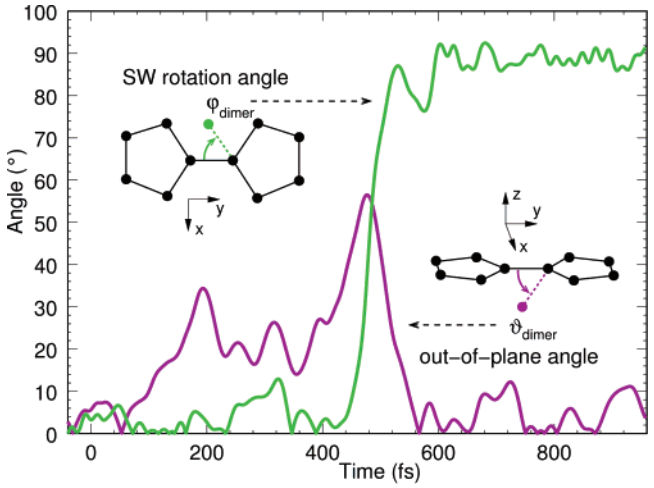

Figure 2. Angles of the SW defect dimer as a function of time. φ_{dimer} corresponds to the angle of the dimer in the plane defined by the two pentagons, ϑ_{dimer} is the tilting angle of the dimer with respect to that plane. As φ_{dimer} goes from 0 to 90° during the inverse SW-type transformation, the tilting angle, ϑ_{dimer}, has a maximum of nearly 60°.

both fixed and variable tube length. In all cases, the excitation threshold for the occurrence of the transition was around $\xi = 7\%$ of the valence electrons. The SW dimer was aligned to the CNT axis in the (7, 7) tube, whereas it was perpendicular to the axis in the (12, 0) tube. These extensive calculations allowed us to draw the following conclusions: (i) laser-induced damage in a CNT with a 5−7−5−7 defect occurs primarily in the defect region (the marked atoms in Figure 1). For laser intensities below the threshold, we find merely enhanced vibrational excitation in the defect region. This low intensity limit was also investigated[19] in a time-dependent density functional study of a single-electron excitation in a defective SWNT where, because of the very low intensity of the excitation, no instability of the 5−7−5−7 defect was observed. (ii) 5−7−5−7 defect elimination depends crucially on the laser-driven CNT expansion and on the bond breaking perpendicular to the SW dimer. This means that 5−7−5−7 defect healing is observed more readily in the (7, 7) CNT at fixed boundary conditions and in the (12, 0) CNT for variable boundary conditions because these two cases show enhanced bond breaking in the SW region during the laser-induced breathing mode.

We have found the damage threshold of SWNTs to vary considerably with tube diameter and chirality.[20] For that reason, in an experiment employing laser pulses to heal defects, care should be taken to determine the damage threshold for the given SWNT ensemble. The laser power used for healing should then be chosen well below the damage threshold.

To investigate the differences between the laser-induced inverse SW-type transformation and the most likely thermally induced mechanism, we have employed a set of ab initio calculations to identify and follow the reaction path from the Stone−Wales defect to the perfect tube. These calculations have been carried out in the framework of density functional theory (DFT) using gradient corrections in the BLYP implementation.[21,22] A Car−Parrinello approach[23] was

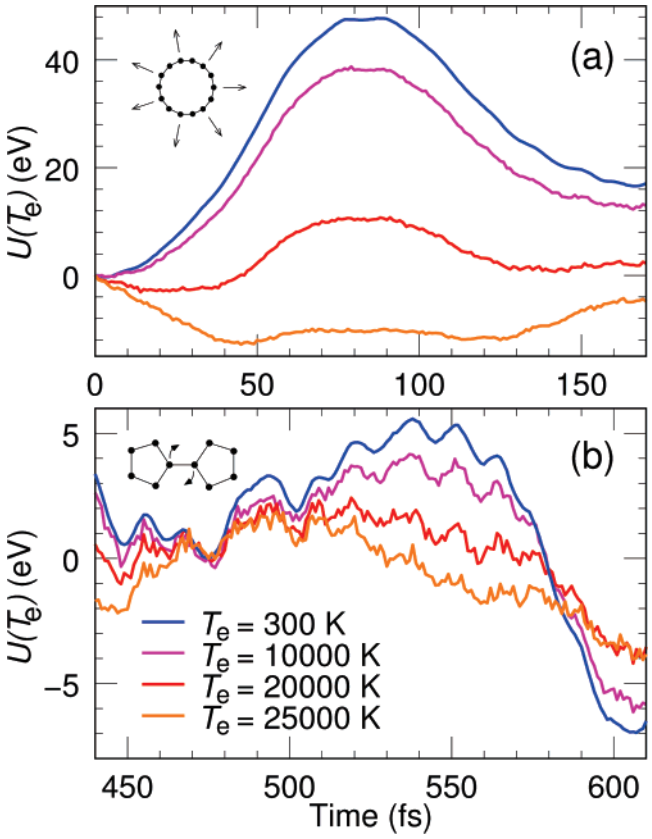

Figure 3. Helmholtz free energy $U(T_e)$ of the electrons along the inverse SW-type transformation path, calculated assuming different electronic temperatures T_e. (a) The large free energy barrier shortly after the laser pulse maximum at $t = 0$ fs corresponds to the first breathing mode of the CNT. The breaking of bonds that are an essential preparation for the SW healing are very costly at $T_e = 300$ K, but energetically favorable at $T_e > 20\,000$ K. (b) The actual rotation of the carbon dimer at $t \approx 450$ fs is prevented by an energy barrier of ∼5 eV at $T_e = 300$ K, but is essentially downhill at $T_e > 20\,000$ K. The free energies were shifted to coincide at $t = 0$ fs in a and at $t = 475$ fs in b.

implemented using an energy cutoff of 40 Ry in a plane wave basis.[23] To determine the energy barrier, we use the climbing image nudged elastic band (CI-NEB) method[24,25] with 16 replicas and a threshold of 0.05 eV/Å for the total force fluctuations. We have considered a unit cell with a (7, 7) half zigzag tube and hydrogen saturated carbons at the tube edges.

We find the minimum energy path shown in Figure 4, with the insets showing initial, transition, and final state structures. The lowest-energy Stone−Wales-type transformation in electronic equilibrium turns out to be an in-plane rotation of the SW dimer around its center of mass. The lattice surrounding the SW dimer undergoes a slight deformation that accommodates the breaking and formation of bonds. The shorter carbon−carbon distance of the dimer in the transition state is due to an intermediate sp hybridization because the SW dimer has lost two bonds with the CNT lattice and has not yet formed two new ones. A very similar reaction path has been reported for fullerenes in ref 16 and also for the case of SW-type transformations in graphite.[15,26] Note that the laser-induced transition, which happens through an out-of-plane dimer rotation, differs dramatically from this in-

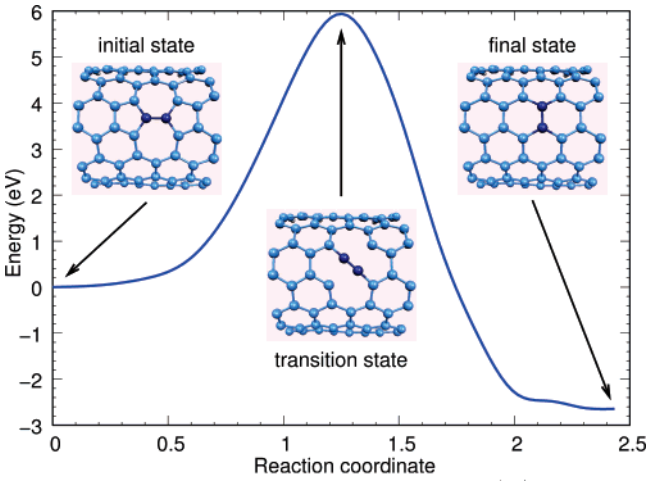

Figure 4. Ab initio calculation of the potential energy barrier between a (7, 7)-CNT with a SW defect and a pure (7, 7)-CNT along the most favorable transition path. The three structure insets show the initial tube with a 5−7−5−7 defect, the transition state which corresponds to the energy maximum along the reaction coordinate, and the final state with the reconstructed 6−6−6−6 lattice. Along its 90° trajectory, the SW dimer contracts slightly from an initial bond length of $d = 1.32$ Å in the SW state to $d = 1.23$ Å at an angle of 45° before expanding to $d = 1.42$ Å in the final state corresponding to the perfect tube. The 45° position is the transition state that is 5.92 eV in energy above the initial state.

plane rotation favored in equilibrium. The differences between thermal and nonthermal 5−7−5−7 defect elimination can be understood as follows. In the ground-state PES, the SW dimer can rotate in-plane via an intermediate sp hybridization involving a bond contraction. Out-of-plane rotation is more expensive energetically because many bonds need to be broken. In contrast, in the laser-excited PES, the interatomic distance within the dimer cannot be reduced because of the presence of electrons in highly antibonding states. In this case, it is more favorable energetically for the dimer to overcome the geometric constraints by rotating out-of-plane after breaking bonds that fluctuate strongly in length because of the RBM and are weakened by the laser excitation. Thus, the laser-induced ultrafast inverse SW-type transformation shown in this paper is not only outstanding because of its extremely nonthermal character but also because of its unusual reaction path.

As shown in Figure 1, the laser-induced structural changes are sharply limited to the 5−7−5−7 defect region for pulses below the pristine CNT ablation threshold. We propose to exploit this localized laser action for nanosurgery in the following way: localized 5−7−5−7 defects would be produced by electron irradiation.[27] Then, an ultrashort laser pulse could be employed to open a CNT in a precisely defined position or affect the coalescence with a second nanoscale object. The ability of femtosecond light pulses to repair defects in CNTs demonstrated in this letter could then be used in a third step to anneal any excess damage. Our preliminary explorations of the femtosecond laser response of Haeckelites nanotubes indicate that laser-induced defect elimination is not limited to the simple SWNT discussed here but can be observed in a large class of nanostructures.

Acknowledgment. M.E.G. acknowledges support by the Deutsche Forschungsgemeinschaft (DFG) through the priority program SPP 1134 and by the European Community Research Training Network FLASH (MRTN-CT-2003-503641). H.O.J. gratefully acknowledges support from the DFG through the Emmy Noether Program. We thank CONACYT-Mexico grants: W-8001-millennium initiative (H.T., M.T.), J-42647-F (A.R.), G-25851-E (H.T., M.T.), 36365-E (H.T.), and 37589-U (M.T.).

References

(1) Chu, M.-W.; Szafraniak, I.; Scholz, R.; Harnagea, C.; Hesse, D.; Alexe, M.; Gösele, U. *Nat. Mater.* **2004**, *3*, 87−90.
(2) Hashimoto, A.; Suenaga, K.; Gloter, A.; Urita, K.; Iijima, S. *Nature (London)* **2004**, *430*, 870−873.
(3) Saito, R.; Dresselhaus, G.; Dresselhaus, M. S. *Physical Properties of Carbon Nanotubes*; Imperial College Press: London, 1998.
(4) Terrones, M. *Annu. Rev. Mater. Res.* **2003**, *33*, 419−501.
(5) Dresselhaus, M. S.; Eklund, P. C. *Adv. Phys.* **2000**, *49*, 705−814.
(6) Stone, A. J.; Wales, D. J. *Chem. Phys. Lett.* **1986**, *128*, 501−503.
(7) Choi, H. J.; Ihm, J.; Louie, S. G.; Cohen, M. L. *Phys. Rev. Lett.* **2000**, *84*, 2917−2920.
(8) Sokolowski-Tinten, K.; Blome, C.; Blums, J.; Cavalleri, A.; Dietrich, C.; Tarasevitch, A.; Uschmann, I.; Förster, E.; Kammler, M.; von Hoegen, M. H.; von der Linde, D. *Nature (London)* **2003**, *422*, 287−289.
(9) Rousse, A.; Rischel, C.; Fournaux, S.; Uschmann, I.; Sebban, S.; Grillon, G.; Balcou, P.; Förster, E.; Gelndre, J. P.; Audebert, P.; Gauthier, J. C.; Hulin, D. *Nature (London)* **2001**, *410*, 65−68.
(10) Jeschke, H. O.; Garcia, M. E.; Bennemann, K. H. *Phys. Rev. Lett.* **2001**, *87*, 015003.
(11) Jeschke, H. O.; Garcia, M. E. Ultrafast structural changes induced by femtosecond laser pulses. In *Nonlinear Optics, Quantum Optics and Ultrafast Phenomena with X-rays*; Adams, B. W., Ed.; Kluwer Academic Publishers: London, 2003.
(12) Xu, C. H.; Wang, C. Z.; Chan, C. T.; Ho, K. M. *J. Phys. Condens. Matter* **1992**, *4*, 6047−6054.
(13) Corio, P.; Santos, P. S.; Pimenta, M. A.; Dresselhaus, M. S. *Chem. Phys. Lett.* **2002**, *360*, 557−564.
(14) Parrinello, M.; Rahman, A. *Phys. Rev. Lett.* **1980**, *45*, 1196−1199.
(15) Kaxiras, E.; Pandey, K. C. *Phys. Rev. Lett.* **1988**, *61*, 2693−2696.
(16) Eggen, B. R.; Heggie, M. I.; Jungnickel, G.; Latham, C. D.; Jones, R.; Briddon, P. R. *Science* **1996**, *272*, 87−90.
(17) Dumitrica, T.; Garcia, M. E.; Jeschke, H. O.; Yakobson, B. I. *Phys. Rev. Lett.* **2004**, *92*, 117401.
(18) Valencia, F.; Romero, A. H.; Jeschke, H. O.; Garcia, M. E. Unpublished work.
(19) Miyamoto, Y.; Rubio, A.; Berber, S.; Yoon, M.; Tom'anek, D. *Phys. Rev. B* **2004**, *69*, 121413(R).
(20) (a) Romero, A. H.; Jeschke, H. O.; Rubio, A.; Garcia, M. E. *Appl. Phys. A* **2004**, *79*, 899. (b) Jeschke, H. O.; Romero, A. H.; Rubio, A.; Garcia, M. E. Unpublished work.
(21) Becke, A. D. *Phys. Rev. A* **1988**, *38*, 3098−3100.
(22) Lee, C.; Yang, W.; Parr, R. C. *Phys. Rev. B* **1988**, *37*, 785−789.
(23) Car, R.; Parrinello, M. *Phys. Rev. Lett.* **1985**, *55*, 2471−2474. We used the code developed by J. Hutter et al. (1990−2003).
(24) Henkelman, G.; Uberuaga, B. P.; Jónsson, H. *J. Chem. Phys.* **2000**, *113*, 9901−9904.
(25) Romero, A. H.; Sbraccia, C.; Silvestrelli, P. L.; Ancilotto, F. *J. Chem. Phys.* **2003**, *119*, 1085−1092.
(26) Xu, C. H.; Fu, C. L.; Pedraza, D. F. *Phys. Rev. B* **1993**, *48*, 13273−13279.
(27) Krasheninnikov, A. V.; Nordlund, K. *Nucl. Instrum. Methods Phys. Res., Sect. B* **2004**, *216*, 355−366.

NL050626T